Supplementary Information (SI) for Journal of Materials Chemistry A.

Truxenone-based donor-acceptor covalent organic framework incorporated with metal sites for enhanced photocatalytic CO_2 reduction

Yanyan Ren, Haiping Liu, Fang Duan*, Shuanglong Lu, Xin Chen, Mingliang Du*

Key Laboratory of Synthetic and Biological Colloids, Ministry of Education, School of Chemical and Material Engineering, Jiangnan University, Wuxi 214122, P. R. China

* Corresponding Authors. E-mail Addresses: duanfang@jiangnan.edu.cn (Fang Duan), du@jiangnan.edu.cn (Mingliang Du)

1. Materials

All commercially available solvents and reagents were purchased with high purity and were used without further purification. 2,7,12-triamino-5H-diindeno [1,2-a:1',2'-c] fluorene-5,10,15-trione (TRO-NH_2), 2, 2'-Bipyridyl-5, 5'-dialdehyde (BPY) were purchased from Jilin Chinese Academy of Sciences-Yanshen Technology Co., Ltd. 4, 4'-Biphenyldicarboxaldehyde (BPD), $NiCl_2$, $ZnCl_2$, $FeCl_3$, $CuCl_2$, trifluoroacetic acid (CF_3COOH), triethylamine (TEA) and triisopropanolamine (TIPA) were purchased from Shanghai Macklin Biochemical Technology Co., Ltd. $Co(NO_3)_2\cdot 6H_2O$, $CoSO_4\cdot 7H_2O$, $Co(OAc)_2\cdot 4H_2O$, $Co(C_5H_8O_2)_2$, $CoCl_2\cdot 6H_2O$ and acetone were purchased from Sinopharm Chemical Reagent Co., Ltd. Tetrahydrofuran (THF), methanol (CH_3OH) , acetonitrile (CH_3CN), 1,2-dichlorobenzene, 1,4-dioxane, N,N-dimethylacetamide (DMAC) and acetic acid (CH_3COOH) were purchased from Shanghai Titan Scientific Co., Ltd. Triethanolamine (TEOA) and tris (2,2'-bipyridine) ruthenium(II) chloride hexahydrate ($[Ru(bpy)_3]Cl_2\cdot 6H_2O$) were purchased from Aladdin.

2. Characterizations

Powder X-ray diffraction (PXRD) data were collected from 2 ° to 30 ° on a Bruker D8 Advance powder X-ray diffractometer. Fourier transform infrared spectroscopy (FT-IR) data were obtained in the frequency range of 4000 to 1000 cm^{-1} on a Thermo Fisher instrument. Solid-state ^{13}C NMR spectra were performed on a Bruker 400M Hz instrument. X-ray photoelectron spectroscopy (XPS) measurements were performed on Thermo Scientific using Kα (hν=1486.6 eV, 300 W) as Monochromatic X-ray source, which were corrected by the binding energy of 284.8 eV of C 1s. N_2 and CO_2 adsorption-desorption isotherms were conducted on Micromeritics ASAP 2460 instrument at 77 K and 278 K, respectively. The pore size distribution was calculated from the nonlocal density functional theory (NLDFT). Thermogravimetric analysis (TGA) was evaluated using a METTLER TGA 2 under nitrogen atmosphere over a temperature range from 50 °C to 800 °C increased at 20 °C min^{-1}. Scanning electron microscopy (SEM) images were obtained from S-4800 equipped EDS detector and transmission electron microscopy (TEM) images were obtained from JEM-2100PLUS at 200 kV. Ultraviolet-visible (UV-Vis) absorption spectra were recorded on a PerkinElmer Lambda 1050+ UV/VIS/NIR Spectrometer. Steady-state photoluminescence (PL) spectra and time-resolved PL spectra of the samples were recorded on Edinburgh FLS1000 spectrophotometer.

3. Photoelectrochemical measurements

All the electrochemical tests were carried out in a standard three-electrode system in 0.5 M Na_2SO_4 using a Hg/Hg_2Cl_2 as the reference electrode, carbon rod as the counter electrode and photocatalysts coated FTO glass as the working electrode by the CHI 760E electrochemical working station. The working electrode was prepared as the following procedure: 3 mg photocatalyst was dispersed in 400 μL isopropanol, and sonicated for half an hour, and then 10 μL Nafion was added. The mixture was taken out and dripped onto the 1x1 cm^2 FTO glass drying to room temperature. Mott Schottky (MS) plots were recorded at different frequencies of 1500, 2000, and 2500 Hz. Electrochemical impedance spectra (EIS) were recorded with the frequency range of

0.01-1000 Hz. The transient photocurrent responses were recorded over an interval of 50 s using a Perfectlight 300W Xenon lamp.

4. Synthesis of COFs

(1) Synthesis of BPD-COF

TRO-NH_2 (21.47 mg, 0.05 mmol) and BPD (15.77 mg, 0.075 mmol) were added into a 10 mL Pyrex tube, and dissolved in 1.5 mL mixed solvents of N, N-dimethylacetamide (DMAC) and 1,4-dioxane (4/1 v/v). The suspension was homogenized by sonication for 30 minutes, and then the acetic acid aqueous (6 M, 25 μL) was added. The tube was flash frozen at 77 K in liquid N_2, which was degassed by three freeze-pump-thaw cycles. Then the tube was sealed under vacuum and heated at 120 °C for 3 days. After cooling down, the precipitate was collected by centrifugation and washed with tetrahydrofuran (THF), acetone and methyl alcohol (CH_3OH) successively. Finally, BPD-COF was obtained by freeze-drying overnight.

(2) Synthesis of BPY-COF

TRO-NH_2 (21.47 mg, 0.05 mmol) and BPY (15.92 mg, 0.075 mmol) were added into a 10 mL Pyrex tube, and dissolved in 3 mL of 1,2-Dichlorobenzene. The suspension was homogenized by sonication for 30 minutes, and then the trifluoroacetic acid aqueous (6 M, 100 μL) was added. The tube was flash frozen at 77 K in liquid N_2, which was degassed by three freeze-pump-thaw cycles. Then the tube was sealed under vacuum and heated at 140 °C for 6 days. After cooling down, the precipitate was collected by centrifugation and washed with acetone until the filtrate was colorless. Finally, BPY-COF was obtained by freeze-drying overnight.

(3) Synthesis of BPY-COF-Co

BPY-COF (30 mg) and $CoCl_2 \cdot 6H_2O$ (100 mg) were added to 20 mL of methanol. The solution was stirred for 8 h at room temperature. The solid was filtered washed with amount of methanol to ensure the removal of residual metal ions and dried in vacuum at 60 °C overnight to obtain BPY-COF-Co. For comparison, BPY-COF-Ni/Zn/Fe/Cu/Co(NO_3)$_2$/$CoSO_4$/Co(OAc)$_2$/Co($C_5H_8O_2$)$_2$ were synthesized similar to the synthetic procedures of BPY-COF-Co. $NiCl_2$, $ZnCl_2$, $FeCl_3$, $CuCl_2$, $Co(NO_3)_2 \cdot 6H_2O$, $CoSO_4 \cdot 7H_2O$, $Co(OAc)_2 \cdot 4H_2O$, and $Co(C_5H_8O_2)_2$ were used to replace of $CoCl_2 \cdot 6H_2O$, and kept other conditions unchanged.

5. Photocatalytic CO_2 reduction experiments

All photocatalytic CO_2 reduction experiments were carried out in a perfectlight 150 mL photoreactor, and the temperature was controlled at 5 °C using a low-temperature constant temperature bath. Detailed experimental procedures were as follows: 10 mg COFs sample, 30 mL acetonitrile, 10 mL sacrificial reagent TEOA and 5 mg photosensitizer $[Ru(bpy)_3]Cl_2 \cdot 6H_2O$ were added into the photoreactor in turn, and the mixture was homogenized by sonication to get a uniformly dispersed solution. Used an automatic online trace gas analysis system to evacuate the photoreactor and fully replaced it with high purity carbon dioxide three times. Afterwards, CO_2 gas was bubbled through the reactor to maintain pressure at 80 kPa, then sealed it without ventilation during the reaction process. For the cyclic experiments, BPY-COF-Co was centrifuged from the reaction mixture, and washed with acetonitrile for 3 times, and then reused in the above-mentioned photocatalytic system. A 300 W Xenon lamp was used as light source. The generated gas in the headspace of the reactor was measured using Fuli 9790II gas chromatography with both TCD and FID detectors. In addition, possible liquid products were detected by ^{1}H NMR spectrum on Bruker AVANCE NEO at 600 MHz.

6. Isotope labeling measurement

The column used in GC-MS was HP-MOLESIEVE (30 m × 0.32 mm, Agilent Technologies, serial number: USD 130113 H). The temperatures of the inlet and oven were 150 and 30 °C, respectively. The carrier gas was nitrogen (N_2) with a flow rate of 1.5 mL·min^{-1}, and the split ratio of carrier gas to sample was set to 10:1.

7. In situ DRIFTS

In situ diffuse reflection infrared Fourier transform spectroscopy (in situ DRIFTS) measurements were conducted on Thermo Fisher Nicolet 6700. The samples were dispersed in acetonitrile with $[Ru(bpy)_3]Cl_2 \cdot 6H_2O$ and TEOA, which were placed in the catalytic reaction chamber equipped with a temperature controller for heating. Firstly, the sample was heated to 100 °C for 2 h under CO_2 flow (30 mL/min) to remove the adsorbed water molecules. After being cooled down to room temperature, the background IR spectra was recorded as a reference in CO_2 atmosphere. Then the acetonitrile was introduced into the chamber via a home-made bubbling system, in which CO_2 flow (10 mL/min) was passed through the acetonitrile at room temperature. After adsorption equilibrium, typical signals of two intermediates were captured after the introduction of flowing CO_2 under dark (30 min) and light irradiation (0-120 min) conditions.

8. Computational Methods

The charge density difference and the change in Gibbs free energy were implemented using the Cambridge sequential total energy package (CASTEP) module of Materials Studio software.[1-3] Exchange-correlation functions were described by generalized gradient approximation (GGA) with Perdew–Burke–Ernzerhof (PBE) pseudopotentials, and the cutoff energy was set to 400 eV. Geometric optimization of all the atomic models was carried out before the energy calculations, and the following convergent tolerances were set: the changes of energy, the maximum stress and the maximum displacement were 2×10^{-5} eV atom^{-1}, 0.1 GPa and 0.002 Å, respectively. To avoid artificial interactions caused by periodicity between adjacent layers in adsorption models, the pristine models were set with 10 Å vacuum layers. The calculation details of the reaction free energy (ΔG) for each step were as follows:[4-5]

$$\triangle G = \triangle E - T \triangle S + \triangle ZPE \tag{1}$$

$$\triangle E=E_2-E_1 \tag{2}$$

where E_1, E_2, $\triangle S$, T, and $\triangle ZPE$ are the energies of the corresponding total energy of the system before reaction step, the total energy of the system after reaction step, the corrective changes in entropy, Kelvin temperature and the corrective changes in zero-point energies, respectively. The lowest unoccupied molecular orbital (LUMO) and the highest occupied molecular orbital (HOMO) were calculated using Dmol^3 code in Materials Studio code to analyze the strength of oxidation and reduction.

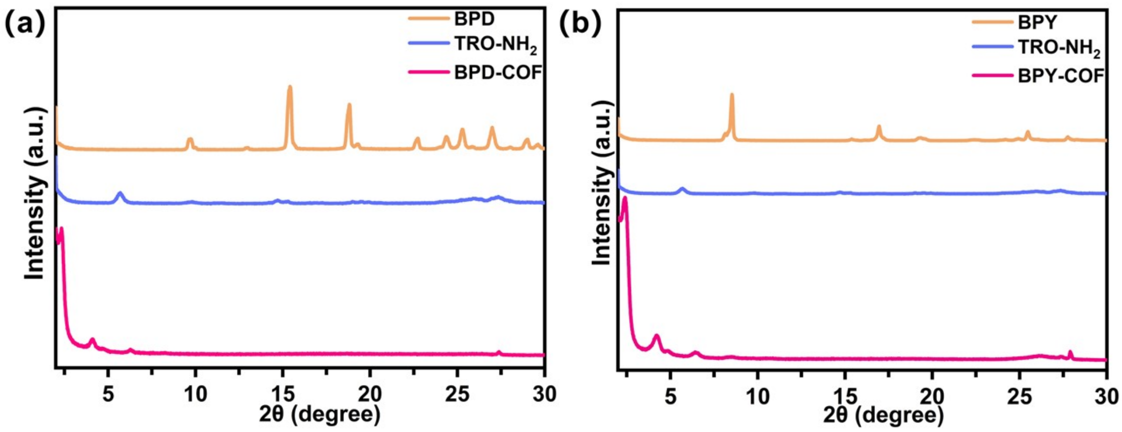

Figure S1. PXRD patterns of (a) BPD-COF and (b) BPY-COF

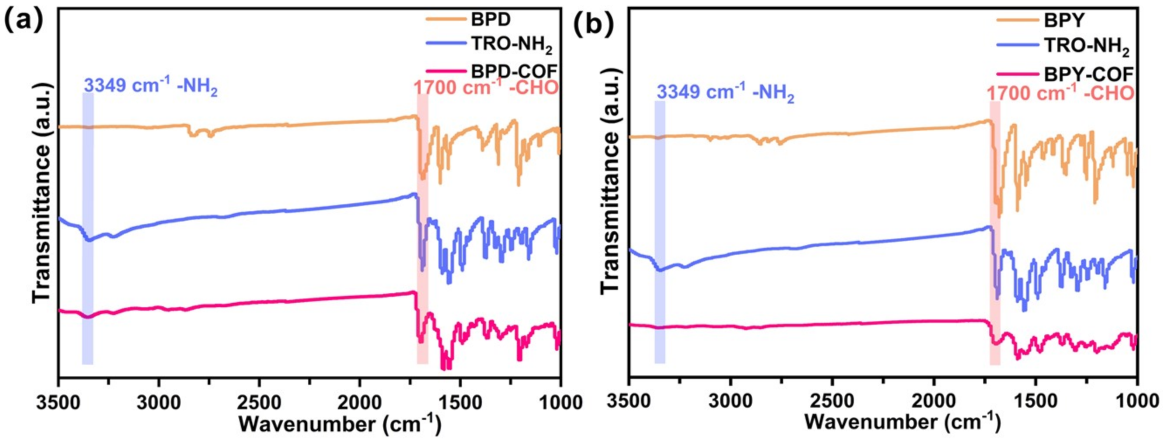

Figure S2. FT-IR spectra of (a) BPD-COF, (b) BPY-COF

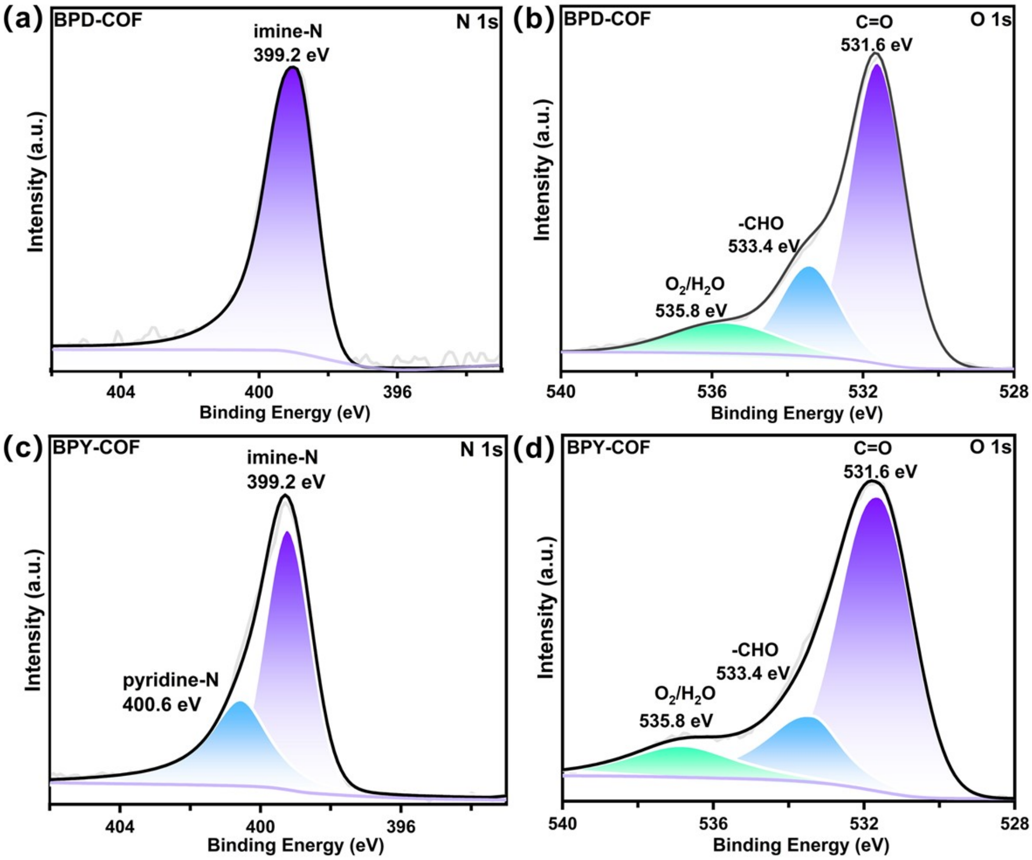

Figure S3. N 1s XPS spectra of BPD-COF (a), BPY-COF (c). O1s XPS spectra of BPD-COF (b), BPY-COF (d)

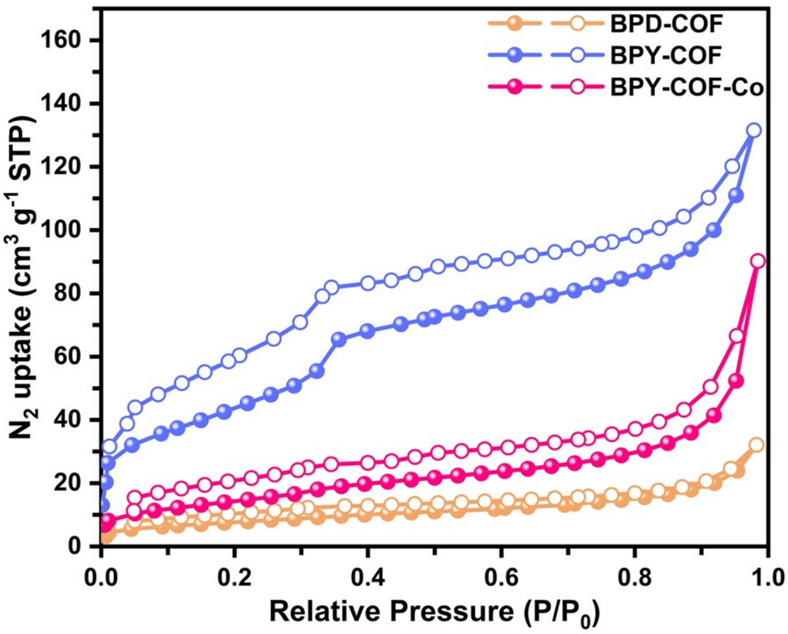

Figure S4. N$_2$ adsorption-desorption curves at 77 K of BPD-COF, BPY-COF and BPY-COF-Co

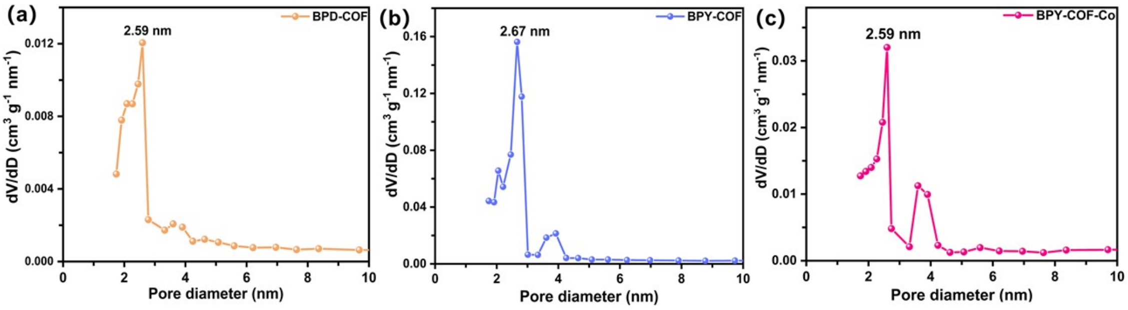

Figure S5. Pore-size distribution curves of BPD-COF (a), BPY-COF (b) and BPY-COF-Co (c)

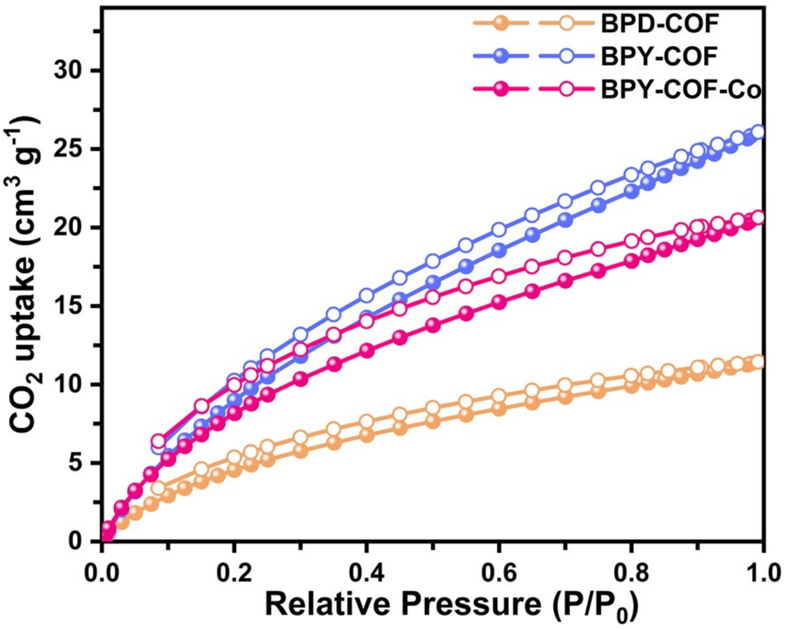

Figure S6. CO$_2$ adsorption-desorption isotherms of BPD-COF, BPY-COF and BPY-COF-Co at 278 K

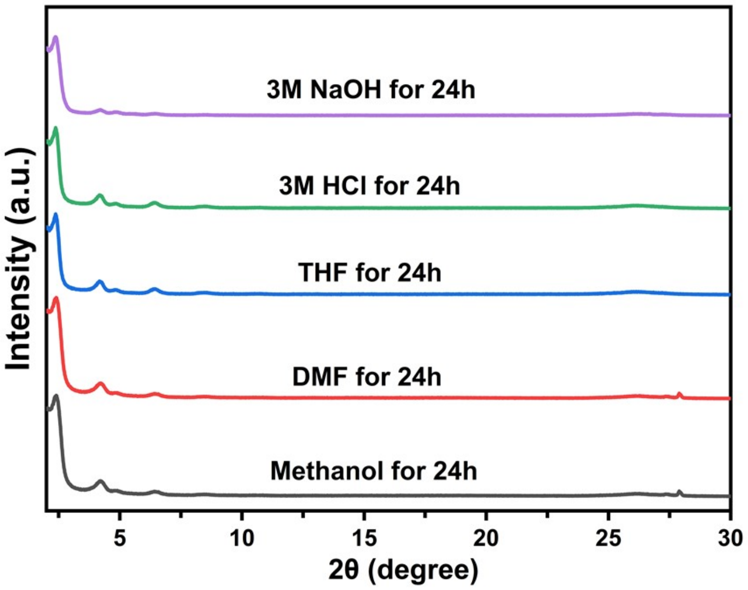

Figure S7. PXRD patterns of BPY-COF-Co in different solvents for 24 h

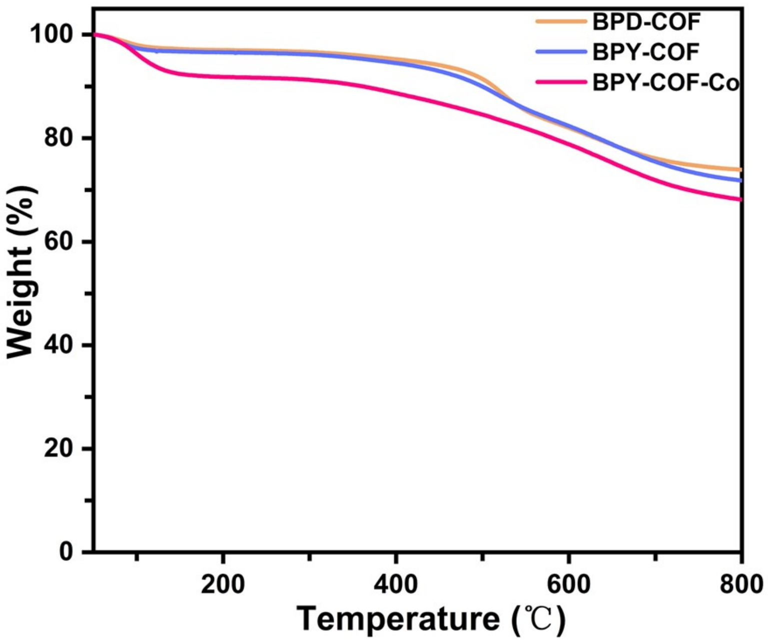

Figure S8. Thermogravimetric curves of BPD-COF, BPY-COF and BPY-COF-Co

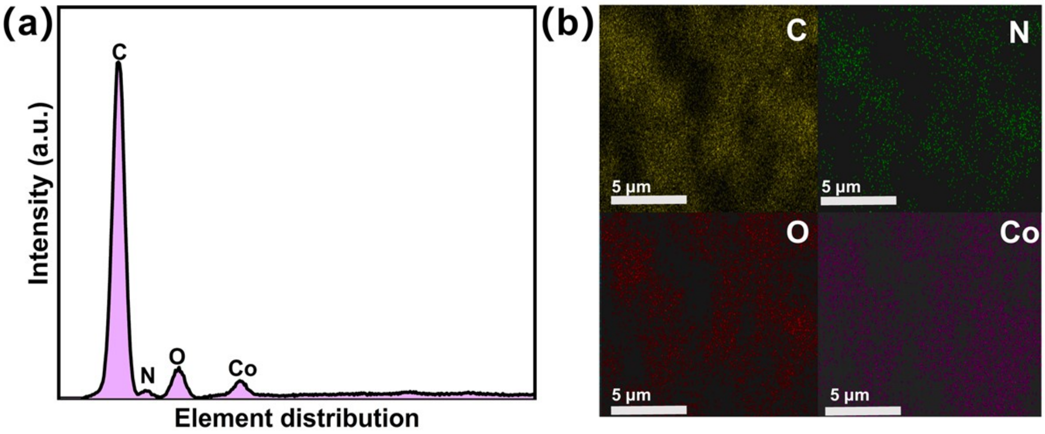

Figure S9. (a) EDX spectrum. (b) The SEM elemental mappings of BPY-COF-Co

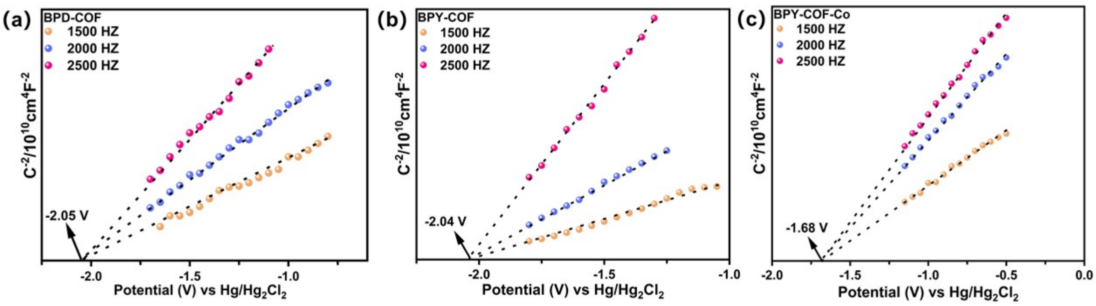

Figure S10. Mott-Schottky plots of (a) BPD-COF, (b) BPY-COF and (c) BPY-COF-Co

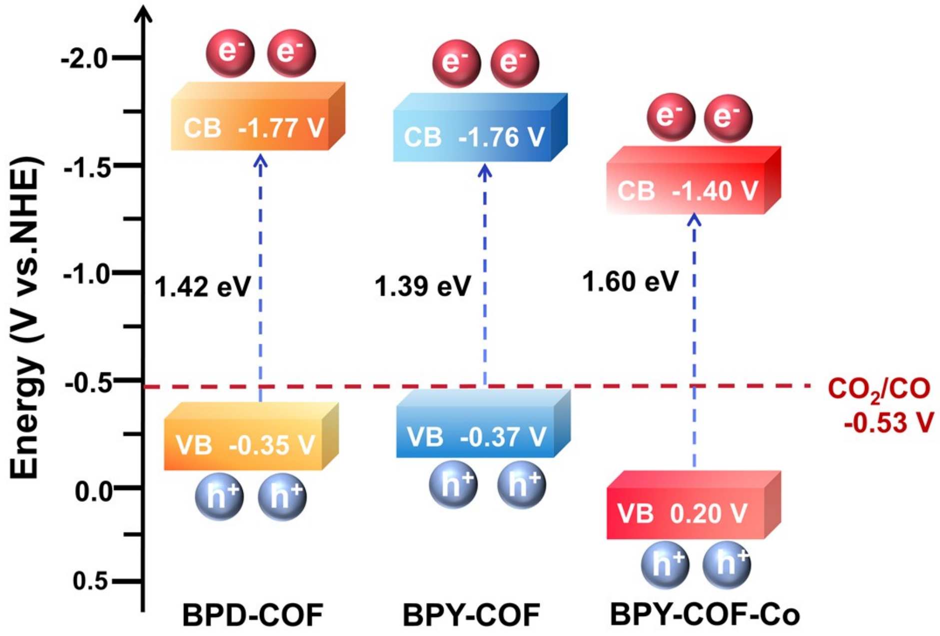

Figure S11. Energy band structures of BPD-COF, BPY-COF and BPY-COF-Co

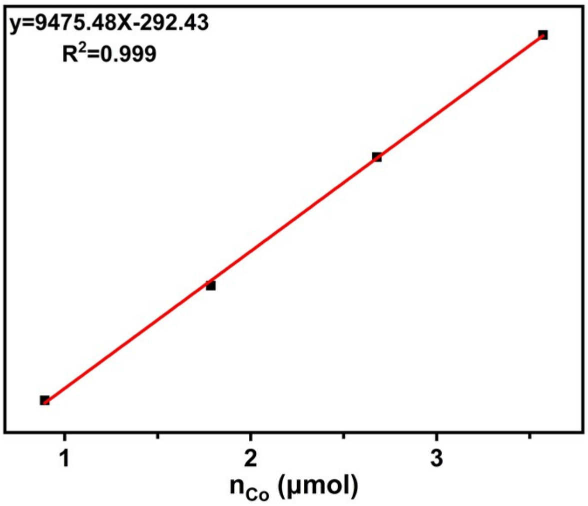

Figure S12. Linear GC calibration curves of CO

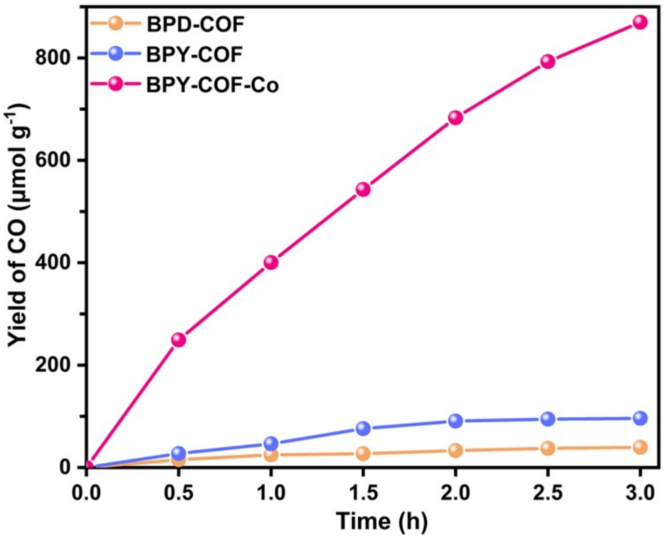

Figure S13. Photocatalytic CO evolution performance as a function of time over BPD-COF, BPY-COF and BPY-COF-Co

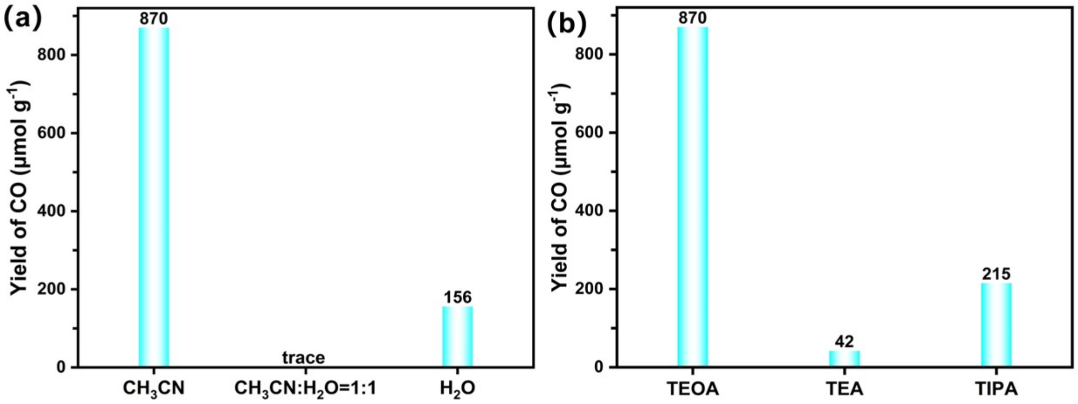

Figure S14. The photocatalytic performance of BPY-COF-Co (a) in different solvent systems and (b) with different sacrificial electron donors

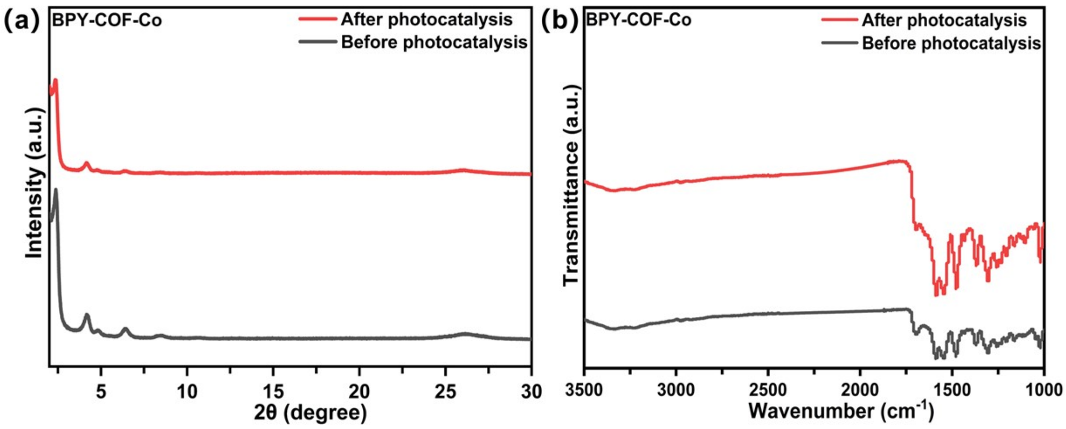

Figure S15. (a) PXRD patterns and (b) FT-IR spectra of BPY-COF-Co before and after photocatalytic reaction

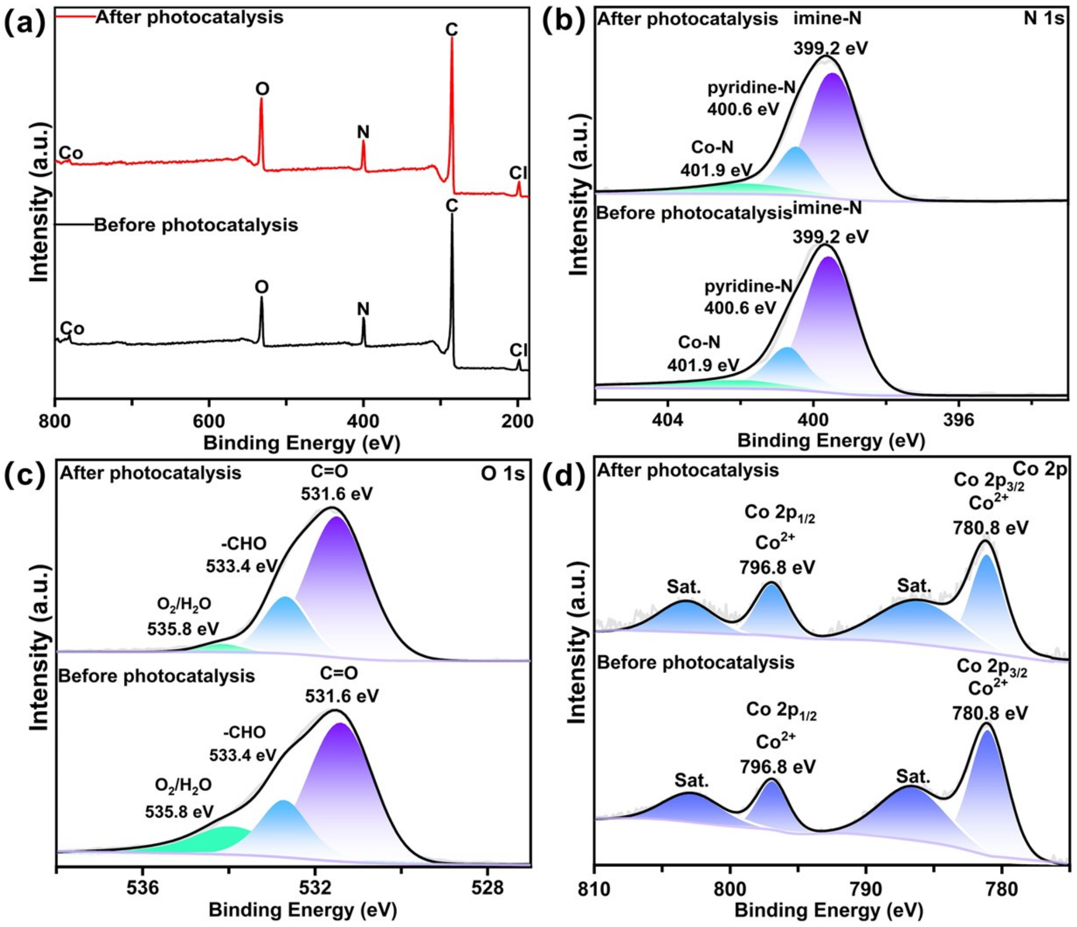

Figure S16. XPS analysis of BPY-COF-Co before and after photocatalytic reaction: (a) survey spectrum, (b)N 1s, (c) O 1s and (d) Co 2p

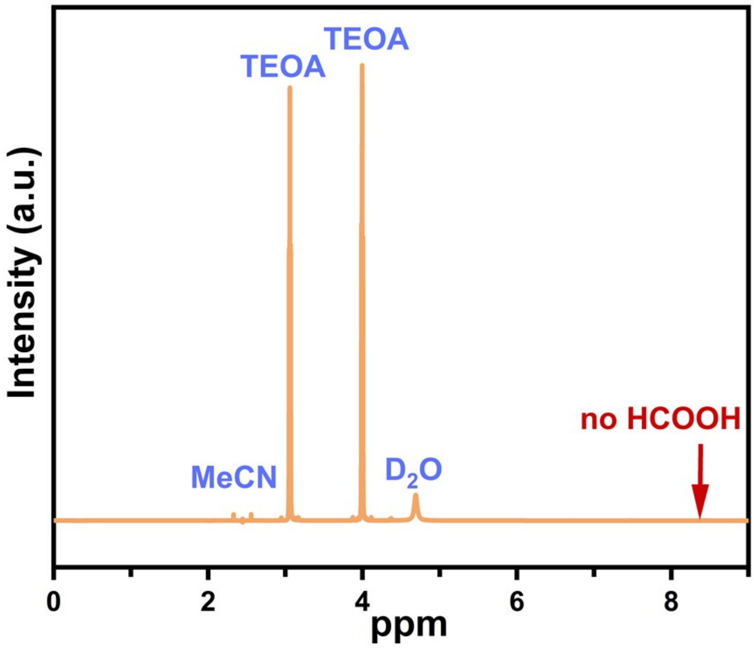

Figure S17. ^{1}H-NMR spectrum of the liquid products after a 3 h CO_2 reduction catalyzed by BPY-COF-Co

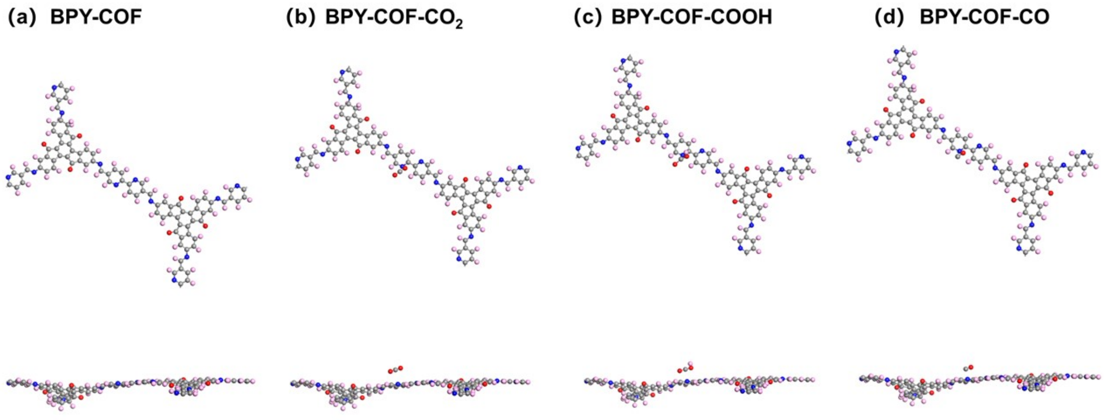

Figure S18. Optimized structure of BPY-COF (a), BPY-COF-CO$_2$ (b), BPY-COF-COOH (c) and BPY-COF-CO (d) under investigation (above is the top view, below is the side view)

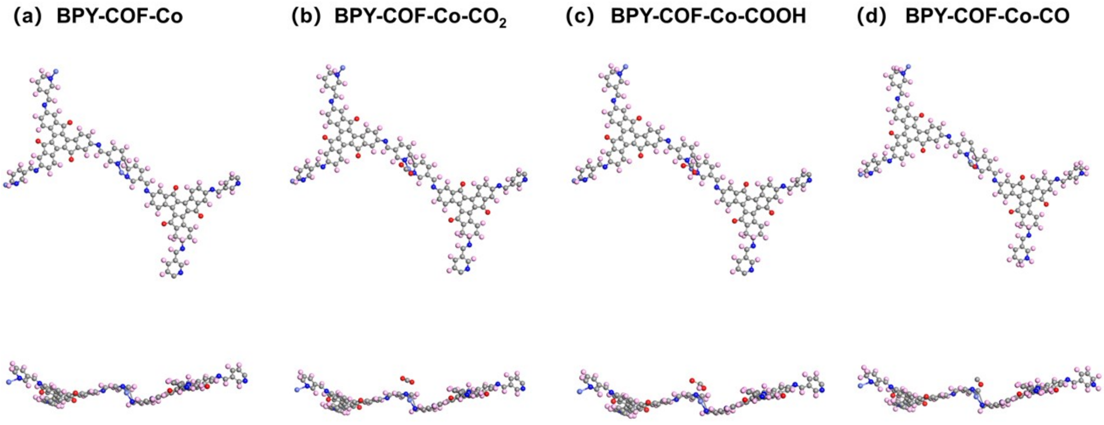

Figure S19. Optimized structure of BPY-COF-Co (a), BPY-COF-Co-CO$_2$ (b), BPY-COF-Co-COOH (c) and BPY-COF-Co-CO (d) under investigation (above is the top view, below is the side view)

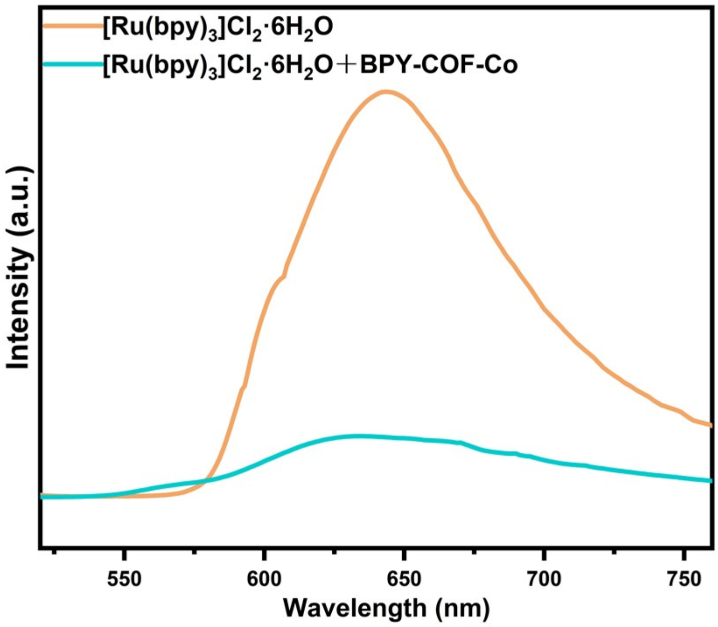

Figure S20. The fluorescence spectra of [Ru(bpy)$_3$]Cl$_2$·6H$_2$O and the mixture of [Ru(bpy)$_3$]Cl$_2$·6H$_2$O and BPY-COF-Co

References

1 Z. H. Li, Y. F. Yan, S. M. Xu, H. Zhou, M. Xu, L. Ma, M. F. Shao, X. G. Kong, B. Wang, L. R. Zheng, H. H. Duan, *Nat. Commun.*, 2022, **13**, 147.

2 C. Liu, M. Y. Han, C. L. Chen, J. Z. Yin, L. L. Zhang, J. Sun, *Nano Lett.*, 2023, **23**, 3507-3515.

3 H. Yousefi-Mashhour, S. Safaeipour, S. Hassani, M. Kalantarian, A. Namiranian, *J. Phys. Chem. C.*, 2024, **128**, 759-767.

4 S. Yang, L. Lu, P. Zhan, Z. H. Si, L. Y. Chen, Y. Zhuang, P. Y. Qin, *Appl. Catal. B.*, 2024, **355**, 124213.

5 M. J. Ding, Z. Q. Wei, D. X. Liu, W. H. Zhao, Q. Lu, Z. M. Li, Q. S. Yu, C. G. Lu, H. Yang, *J Energ. Chem.*, 2025, **101**, 598-607.